

Conference Proceedings Paper

Sensitive *versus* Rough Dependence in Initial Conditions in Atmospheric Flow Regimes

Anthony R. Lupo ^{1,*} and Yanguang Li ²

Published: 19 July 2016

¹ Department of Soil, Environmental, and Atmospheric Sciences, University of Missouri, Columbia, MO, USA

² Department of Mathematics, University of Missouri, Columbia, MO, USA

* Correspondence: lupoa@missouri.edu

Abstract: In this work, we will identify the existence of 'rough dependence on initial conditions' in atmospheric phenomena, a concept which is a problem for weather analysis and forecasting. Typically, two initially similar atmospheric states will diverge slowly over time such that forecasting the weather using the Navier-Stokes equations is useless after some characteristic time-scale. With rough dependence, two initial states diverge quickly implying forecasting is impossible. Using previous research in atmospheric science, rough dependence is characterized by using quantities that can be calculated from atmospheric data. Rough dependence will be identified in atmospheric phenomena on different time scales. The nature of rough dependence will be studied using a research model. Data was provided for this project by archives outside MU, and using our MU RADAR at the South Farm experiment station.

Keywords: rough dependence on initial conditions; sensitive dependence on initial conditions; RADAR; blocking

1. Introduction

In atmospheric sciences, weather forecasters today rely on numerical models in order to make predictions (synoptic-scale), and these can be made reliably out to about seven days, sometimes quite well (e.g., Winter Storm Jonas 22–23 January, 2016–impacted the Eastern USA) but the absolute limit is about 10–14 days. However, numerical weather forecasts on the same space scale can fail in the one to two day time frame, or even more quickly (e.g., Tropical Cyclone Patricia 22–23 October, 2015–Eastern Pacific Ocean basin). The general reason for their failure is threefold, and these are; (a) incomplete knowledge of physical processes (parameterization–e.g., latent heat); (b) lack of data, and (c) measurement error (e.g., [1,2]). Then, error in the initial and/or boundary conditions can render model forecasts as quickly as a few days [3], and this behavior which is inherent in the Navier Stokes equations is called sensitive dependence on the initial conditions (SDOIC) [4]. On smaller scales, predictability has improved greatly in the last 20 years, which has saved lives and property. However, smaller-scale systems can also change radically on very small time scales (e.g., 5–10 min) as detected by RADAR.

One way that the forecasting community can mitigate or qualitatively represent SDOIC in weather forecast model output is through the use of ensemble modeling techniques (e.g., [5–7]), and an example of these kind of operational products can be found at (<http://www.esrl.noaa.gov/psd/map/images/ens/ens.html#nh>). Ensemble modeling techniques were produced at the National Centers for Environmental Prediction (NCEP), and have been in use for more than two decades [7]. The NCEP forecasts are produced using 17 different runs of the global model using the initial

conditions and initial conditions that are assumed to be within the range of analysis error. Then, the ensemble mean performs better typically than any of the individual runs. The most widely used ensemble products choose representative contours at 500 hPa, and plots all of these realizations on a map. These are called “spaghetti plots”, since the contours will look like a plate of spaghetti after some period of time when the forecasts diverge. Often, but not always, when the spread among the ensembles is small, forecasts are more skillful.

In the study of atmospheric phenomena, the behavior of the fluid on different time and space-scales using the Navier-Stokes equations is elucidated through the use of scaling parameters. For example, the assumption that the atmosphere is close to being geostrophically balanced can be represented using the Rossby Number (e.g., [8]), which is the ratio of the fluid acceleration (difference between pressure gradient force and Coriolis force) and the inertial (Coriolis) forces. If the Rossby number is zero, the atmosphere is geostrophically balanced, although this is an ideal condition that assumes the atmosphere is inviscid and steady state. However, there is always some departure from geostrophy in the observed atmosphere (e.g., [9]). The Reynolds number is the ratio between the inertial to viscous forces. If the Reynolds Number is large, the atmospheric flow is three-dimensional and dominated by inertial forces, as such, a flow possess turbulence as represented by eddies and vortices. Low Reynolds Number flows are laminar (two dimensional) and viscous forcing is dominant. Using the Reynolds Number, a characteristic time scale for a flow can be derived. If the growth period of an atmospheric disturbance is larger than that implied by the characteristic time scale, then SDOIC will characterize the forecast of the system and these forecasts represented by trajectories (or contours in the ‘spaghetti plots’) will diverge slowly with time. If the time period for growth is less than the characteristic time scale, then trajectories will diverge exponentially with time and this implies that predictability is not possible. In this case, the flow is roughly dependent on the initial conditions (RDOIC) [10,11].

Rough dependence on initial conditions is a new theory about the nature of turbulence in fluid flows [10,11], under the conditions of a large Reynolds number. Fluid dynamics has long suspected that turbulence is more than just a chaotic flow. Like SDOIC, RDOIC occurs in an ensemble where the initial conditions of each member are very similar, except that where in SDOIC their divergence occurs slowly with time, in RDOIC, the trajectories diverge very rapidly [10]. This theory also states that in high Reynolds number flows RDOIC represents ‘violent’ turbulence [10]. In a meteorological context, unpredictable and rapidly growing phenomena are said to undergo ‘explosive’ development (e.g., [12]). However, there is no discussion as of yet of RDOIC in the atmospheric science literature. Thus, the goal of this work is to demonstrate the existence of RDOIC in examples of both large-and smaller-scale atmospheric phenomena, and differentiate this from SDOIC. In accomplishing this task, we will develop methods for quantifying this in atmospheric flows in section two. Case studies will be presented in section three, and a summary and conclusions will be present in section four.

2. Data and Methods

2.1. Data

In order to meet our objectives, several data sets will be used. These will be RADAR data archived from the University of Missouri RADAR located at South Farm research station. This data is readily available from the RADAR Applications, Instrumentation, And Nowcasting Systems (RAINS) lab participating in the EPSCoR project, and which is available in decibel levels (DBZ). Here we will identify coherent features as those at 30 DBZ or more. Also, the National Centers for Environmental Prediction/National Center for Atmospheric Research (NCEP/NCAR) re-analyses, archived at the NCAR research facilities in Boulder, CO, USA (<http://www.esrl.noaa.gov/psd/data/reanalysis/reanalysis.shtml>) can be used which provide for large-scale meteorological data at various resolutions from $1^\circ \times 1^\circ$ to $2.5^\circ \times 2.5^\circ$ latitude-longitude grids.

2.2. Methods

SDOIC occurs in a system where at least one Lyapunov Exponent is positive, and as stated above it is a measure of divergence for the trajectories of two systems that are initially close. SDOIC also demonstrates the presence of chaos. The Lyapunov Exponent is defined as the characteristic exponent in the solution of a differential equation and is expressed as:

$$\lambda_i = \lim_{t \rightarrow \infty} \left\{ \lim_{\varepsilon(0) \rightarrow 0} \left[\frac{1}{t} \ln \left(\frac{\varepsilon_i(t)}{\varepsilon(0)} \right) \right] \right\}, i = 1, \dots, n \quad (1)$$

where λ_i is the i th Lyapunov Exponent of an n -dimensional system. In the atmosphere, [13] postulated that if the atmosphere is barotropic, the positive Lyapunov Exponent in the atmosphere can be expressed as the area integrated regional enstrophy (IRE):

$$\sum_{i>0} \lambda_i \approx \int_A \zeta^2 dA \quad (2)$$

Where ζ is the vorticity, or the curl of the wind vector and the quantity squared is called enstrophy, which is the dissipation tendency of a fluid. The work of [14] demonstrated the utility of this quantity in identifying the onset and termination of atmospheric blocking and flow regime transformation. As a positive Lyapunov Exponent, this quantity relates to predictability and can also be related to Kolmogorov Entropy (or metric entropy) (e.g., Ott, 1993). The larger the IRE, the less predictable the atmosphere, as trajectories of two initial conditions would diverge rapidly.

In [10], RDOIC is defined using (1) and representing short term rapid growth as (using the notation of Equation (1)):

$$\lambda_r = \lim_{t \rightarrow 0^+} \frac{1}{t^\alpha} \left(\frac{x(t)}{x(0)} \right) \quad (3)$$

where the Lyapunov Exponent represents rapid growth over a short time, under the condition that the exponent $\alpha > 0$. Then Li [10] applies this principle in the Navier-Stokes equation in order to estimate the temporal growth of modes in the equation, and the result is (for more detail, see [10]);

$$x(t) \leq e^{C\sqrt{tRe} + C_1 t} (X(0)) \quad (4)$$

where Re is the Reynolds number as defined in Section 1, t is time and C and C_1 are defined in [10]. Thus, this implies exponential growth with the square root of time and the Reynolds number that is larger than that implied by the Lyapunov Exponent, or violent turbulence is RDOIC. Then, using Equation (2) and substituting into (3) for the Lyapunov Exponent, and comparing to (4) we can define RDOIC in terms of quantities that can be measured and then calculated directly from an atmospheric flow. RDOIC can be estimated as:

$$\int_A \zeta^2 dA \leq C\sqrt{tRe} + C_1 t \quad (5)$$

a newly derived expression that can be used to evaluate the presence of RDOIC versus SDOIC in terms of atmospheric phenomena. In Equation (5) above the constants C and C_1 are (see [10]):

$$C = \frac{8}{\sqrt{2}e} \max_{\tau \in [0, T]} \|u(\tau)\|_n \quad (6a,b)$$

$$C_1 = 4 \max_{\tau \in [0, T]} \|u(\tau)\|_n - \frac{\sqrt{2}e}{2} C$$

In Equation (5) above, vorticity (ζ) can be calculated by taking the curl of the wind vector, or since vorticity can be defined as circulation per unit area;

$$\zeta \equiv \left(\frac{\partial v}{\partial x} - \frac{\partial u}{\partial y} \right) \equiv \lim_{\Delta A \rightarrow 0} \left(\frac{\Delta C}{\Delta A} \right) \quad (7)$$

where Δc is some change in circulation and ΔA the change in area, and in Equation (7), we can estimate Δc as;

$$C \equiv \oint \vec{V} \cdot d\vec{r} \approx \sum \vec{V}_h \cdot \Delta \vec{r} \equiv \Delta C \quad (8)$$

where V is the velocity vector, and r —the position vector.

3. Results

3.1. Case Study, Blocking

The blocking event examined here occurred during 23 January to 16 February 2014 and was located over the Eastern Pacific near the Gulf of Alaska and near the West Coast of North America (130° W) (see <http://solberg.snr.missouri.edu>). This event formed out of a very long-lived ridge over the same area. The event dominated a significant period of the winter season, and was likely responsible for the cold winter over North America that year (e.g., [15]). The work of [16] describes this event in more detail and the 500 hPa heights during the intensification stage of the blocking event which is shown in Figure 1. This event was noteworthy as it survived a large-scale flow regime change during early February 2014 (4th–7th), as the Pacific North American (PNA) teleconnection pattern change from positive to negative during early February 2014. Earlier work (e.g., [17,18]) suggested that blocking events would not survive a transition in the large-scale flow regime, and [16] showed that, under certain conditions, these events could survive. Additionally, this event is noteworthy for the longevity and persistence.

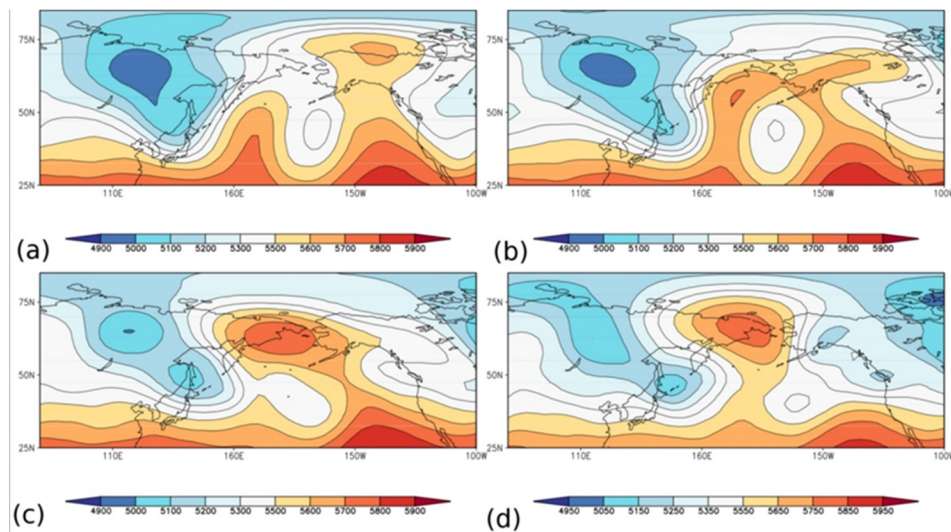


Figure 1. Adapted from [16], the 500 hPa heights derived from the NCEP/NAR reanalyses over the Pacific Ocean basin at 1200 UTC for (a) 4 February; (b) 5 February; (c) 6 February; and (d) 7 February in 2014.

Examining the block intensity (BI) [19] for this case (Figure 2a) demonstrated that the block was more intense just following the onset of the event, and then intensified in early February (3rd–6th) near the same time that the phase of the PNA flipped from positive to negative indicating flow regime change. Then, BI was markedly less indicating a weaker block until the decay period. The IRE diagnostic also followed a similar evolution during the block lifecycle (Figure 2b), with the IRE maximizing during onset, intensification, and termination. Then a calculation using In Equation (5) demonstrates that this blocking event would be a large-scale event, and the dynamics are dominated by quasi-geostrophic processes (e.g., [8,9]) and SDOIC dynamics. The value calculated using the IRE in the Northern Hemisphere on the left-hand-side ($\sim 6.5 \times 10^8$) is of similar magnitude to that

calculated using the Reynolds Number and constant C on the right-hand-side ($\sim 5 \times 10^8$). Recall, that [10] argued that RDOIC would exist if the time-scale for the growth and evolution of a system is smaller than that implied by the Reynolds number ($\sim 2.3 \times 10^8$) for a synoptic-scale flow (length-scale–5000 km, time-scale 10^5 s), and blocking can be characterized as a similar scale phenomenon.

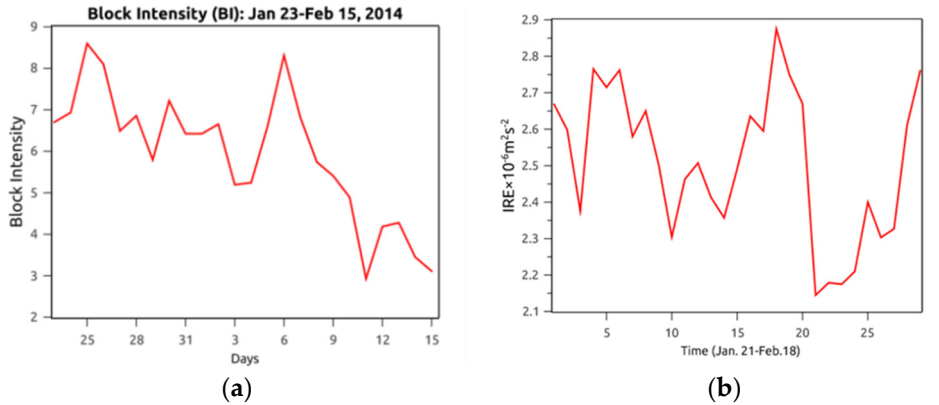


Figure 2. Adapted from [16], (a) the Block Intensity (BI) from [19] (ordinate) for the event studied in winter 2014 versus date in January and February 2014 (abscissa) (left); and (b) the IRE(s^{-2}) (ordinate) and days following the onset period in January and February 2014 (abscissa) (right).

3.2. Case Study, Hurricane Patricia

Hurricane Patricia was an intense (Category 5 on the Saffir-Simpson Scale) Eastern Pacific tropical cyclone which occurred in late October 2015 and moved inland over western Mexico as a Category 5 event (Figure 3). This hurricane formed out of a tropical depression over the southeast Pacific Ocean Basin (<http://weather.unisys.com>), and was classified as a tropical storm early (0300 UTC) on 21 October 2015, with a central pressure of 1004 hPa. Patricia became a hurricane approximately 30 hr later, and reached maximum intensity ($\sim 100 \text{ m}\cdot\text{s}^{-1}$) 24 h after becoming a hurricane with a central pressure of 880 hPa making it the most intense storm by that measure in the Eastern Pacific Ocean Basin. The total pressure fall was 124 hPa in 42 h ($3.0 \text{ hPa}\cdot\text{h}^{-1}$), which given the low-latitude ($\sim 20^\circ \text{ N}$), is nearly 7.5 times the rate for the definition of explosive cyclogenesis published by [20]. Most of the pressure fall (100 hPa) occurred during a 24-h period from 0900 UTC 22 October to 0900 UTC 23 October 2015, and this rate is more than 10 times the rate for explosive cyclogenesis.

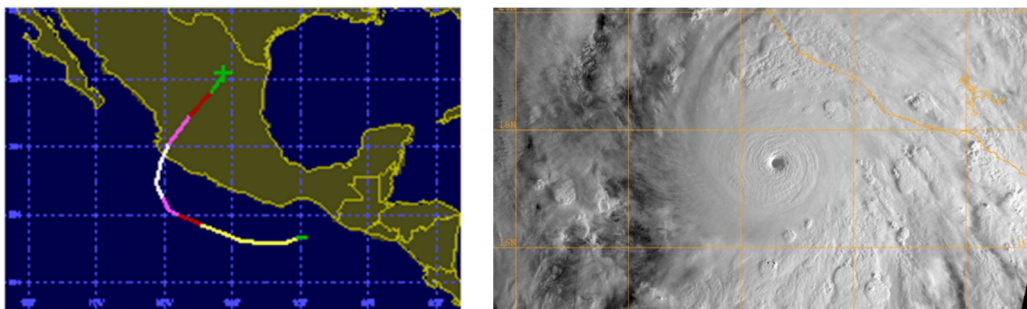


Figure 3. The track of Hurricane Patricia (see: <http://weather.unisys.com>) (left), and a visible satellite image near the time for maximum intensity at 1500 UTC 23 October, 2015 (right).

This development rate is more consistent with mesoscale phenomena, and the development of tropical cyclones is recognized to be comprised of several mesoscale convective systems (MCVs) (e.g., [21]). Additionally, intense tropical cyclone environments cannot reasonably be described as geostrophic. The eyewall is frequently non-hydrostatic and models of these environments use gradient wind (e.g., [22]). Calculations using In Equation (5) were carried out by considering Hurricane Patricia as a synoptic-scale entity in a large-scale environment. The

right-hand-side in this case is about four times that left-hand-side indicating RDOIC dynamics or violent turbulence [10]. If Hurricane Patricia is considered a mesoscale feature in a mesoscale environment, the right-hand-side is an order of magnitude larger.

Hurricane track prediction has substantially improved in recent years, and the model forecasts issued near the time for the commencement of rapid deepening for the track of Patricia performed very well (Figure 4). At this time Patricia was classified as a tropical storm. The intensity of Patricia was not well forecast, however, as the suite of models forecast maximum intensity to occur 36 hr later, with maximum winds at just more than half ($50\text{--}55\text{ m}\cdot\text{s}^{-1}$ versus $100\text{ m}\cdot\text{s}^{-1}$) and a central pressure much higher ($950\text{--}960\text{ hPa}$ versus 880 hPa) than observed. Thus, even with rapid deepening about to commence, the suite of models which are tuned specifically for hurricane forecasting (e.g., the Hurricane Weather Research Forecast (HWRF) model). This forecast represents a dramatic example of the problems inherent in forecasting smaller –scale events.

4. Conclusions

The objectives of this study were to determine whether RDOIC exists in observed atmospheric phenomena and to develop a relationship to diagnose RDOIC as a function of observable atmospheric quantities. This relationship was developed in Section 2. Then using observed atmospheric data for a long-lived blocking event and Hurricane Patricia, In Equation (5) was used to determine whether or not these cases were governed by quasi-geostrophic and SDOIC or RDOIC dynamics.

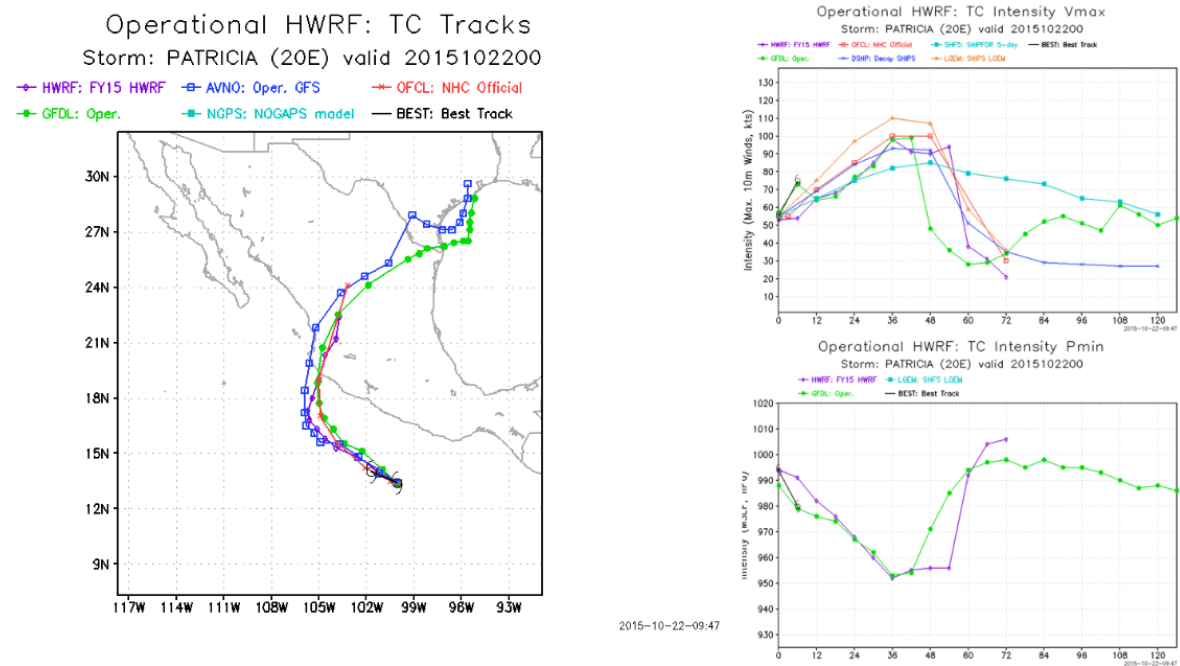


Figure 4. Forecast products available at 0000 UTC 22 October 2015 to the operational community for Hurricane Patricia. The left-hand-side diagram is the track prediction for Hurricane Patricia, the right hand side is the maximum wind speed (upper), and the central pressure (lower).

While blocking can develop very rapidly and models fail to anticipate their onset and/or decay [23], the results here suggest that the long-lived, Pacific Region winter blocking event of 2014 was likely governed by quasi-geostrophic and SDOIC dynamics. The space and time-scale for blocking in general is consistent with that of the synoptic and planetary-scales. The results here suggest that predictability for this type of event is at least possible in a weather forecast model.

In the case of Hurricane Patricia, an extremely rapidly developing event, the numerical models failed to predict the intensity the storm would attain within 24 h of the onset of rapid deepening. The

model forecasts were not aggressive or fast enough in predicting the storms final severity. Hurricane Patricia likely developed at a rate consistent with convective-scale phenomena (meso- β or γ), and the calculation using In Equation (5) demonstrated the presence of RDOIC dynamics.

It could be argued that the excessive deepening of Hurricane Patricia occurred as the result of excessive latent heat release [21,22], which is not represented in simplified versions of the NS equations. Thus, it might be difficult to differentiate SDOIC and RDOIC here. The work of [11] extended that of [10] to include viscous effects and found solutions to the NS equations. Also, [9] showed that latent heat release feeds back on the ageostrophic component of motion in the atmosphere, and thus is included in the observed velocity used in the calculations here. In future work, as suggested in section two, RADAR data will be examined in order to detect RDOIC in convective phenomena.

Acknowledgments: The authors would like to acknowledge the anonymous reviewers of this work.

Conflicts of Interest: The authors declare no conflict of interest. The founding sponsors had no role in the design of the study; in the collection, analyses, or interpretation of data; in the writing of the manuscript, and in the decision to publish the results.

References

1. Haltiner, G.J.; Williams, R.T. *Numerical Prediction and Dynamic Meteorology*, 2nd ed.; Wiley and Sons, Inc.: Chichester, UK, 1980; p. 477.
2. Durrant, D.R. *Numerical Methods for Wave Equations in Geophysical Fluid Dynamics*; Springer-Verlag, Inc.: New York, NY, USA, 1999; p. 463.
3. Lorenz E.N. Deterministic, non-periodic flow. *J. Atmos. Sci.* **1965**, *20*, 130–141.
4. Lorenz, E.N. A study of the predictability of a 28-variable model. *Tellus* **1963**, *17*, 321–333.
5. Toth, Z.; Kalnay, E. Ensemble forecasting at NCEP: The generation of perturbations. *Bull. Am. Meteorol. Soc.* **1993**, *74*, 2317–2330.
6. Toth, Z.; Kalnay, E. Ensemble forecasting at NCEP and the breeding method. *Mon. Weather Rev.* **1997**, *125*, 3297–3319.
7. Tracton, M.S.; Kalnay, E. Ensemble forecasting at the National Meteorological Center: Practical Aspects. *Weather Frcst.* **1993**, *8*, 379–398.
8. Holton, J.R.; Hakim, G.J. *An Introduction to Dynamic Meteorology*; Academic Press, Elsevier: Amsterdam, The Netherlands, 2012; p. 532.
9. Lupo, A.R. The role of ageostrophic forcing in a Height Tendency Equation. *Mon. Weather Rev.* **2002**, *130*, 115–126.
10. Li, Y.C. Distinction of turbulence from chaos—rough dependence on initial data. *Electr. J. Differ. Eq.* **2014**, 1–8.
11. Li, Y.C. Rough dependence upon initial data exemplified by explicit solutions and the effect of viscosity. **2016**, in press.
12. Lupo, A.R.; Smith, P.J.; Zwack, P. A diagnosis of the development of two extratropical cyclones. *Mon. Wea. Rev.* **1992**, *120*, 1490–1523.
13. Dymnikov, V.P.; Kazantsev, Y.V.; Kharin, V.V. Information entropy and local Lyapunov exponents of barotropic atmospheric circulation. *Izv. Atmos. Ocean. Phys.* **1992**, *28*, 425–432.
14. Jensen, A.D.; Lupo, A.R. Using enstrophy based diagnostics in an ensemble for two blocking events. *Adv. Meteor., Special Issue: Large scale dynamics, anomalous flows, and teleconnections Atmospheric Science*, **2013**, 7pp, Article ID 693859.
15. Quiroz, R.S. The climate of the 1983–1984 winter: A season of strong blocking and severe cold in north America. *Mon. Weather Rev.* **1984**, *112*, 1894–1912.
16. Jensen, A.D. A dynamic analysis of a record breaking winter season blocking event. *Adv. Meteor., Special Issue: Large scale dynamics, anomalous flows, and teleconnections Atmospheric Science*, **2015**, 2015, 9, Article ID 634896.
17. Haines, K.; Holland, A.J. Vacillation cycles and blocking in a channel. *Q. J. R. Meteorol. Soc.* **1998**, *124*, 873–897.

18. Lupo, A.R.; Mokhov, I.I.; Dostoglou, S.; Kunz, A.R.; Burkhardt, J.P. Assessment of the impact of the planetary scale on the decay of blocking and the use of phase diagrams and enstrophy as a diagnostic. *Izv. Atmos. Ocean. Phys.* **2007**, *43*, 45–51.
19. Wiedenmann, J.M.; Lupo, A.R.; Mokhov, I.I.; Tikhonova, E.A. The climatology of blocking anticyclones for the Northern and Southern Hemispheres: Block intensity as a diagnostic. *J. Clim.* **2002**, *15*, 3459–3473.
20. Sanders, F.; Gyakum, J.R. Synoptic-dynamic climatology of the “bomb”. *Mon. Weather Rev.* **1980**, *108*, 1577–1589.
21. Houze, R.A. Clouds in tropical cycles. *Mon. Weather Rev.* **2010**, *138*, 293–344.
22. Schubert, W.H.; Montgomery, M.T.; Taft, R.K.; Guinn, T.A.; Fulton, S.R.; Kossin, J.P.; Edwards, J.P. Polygonal eyewalls, asymmetric eye contraction, and potential vorticity mixing in hurricanes. *J. Atmos. Sci.* **1999**, *56*, 1197–1223.
23. Matsueda, M. Predictability of Euro-Russian blocking in summer of 2010. *Geophys. Res. Lett.* **2011**, *38*, 6, L06801.



© 2016 by the authors; licensee MDPI, Basel, Switzerland. This article is an open access article distributed under the terms and conditions of the Creative Commons by Attribution (CC-BY) license (<http://creativecommons.org/licenses/by/4.0/>).